J Appl Electrochem (2010) 40:2185–2191
DOI 10.1007/s10800-010-0200-0

ORIGINAL PAPER

Non-woven fabric supported poly(acrylonitrile-vinyl acetate) gel electrolyte for lithium ion battery use

**Xiaoping Li · Mumin Rao · Youhao Liao ·
Weishan Li · Mengqing Xu**

Received: 21 January 2010 / Accepted: 5 September 2010 / Published online: 17 September 2010

Abstract This paper reported on a new gel polymer electrolyte (GPE) based on polyethylene (PE) non-woven fabric supported poly(acrylonitrile-vinyl acetate) (P(AN-VAc)/PE) membrane for lithium ion battery use. The preparation and performances of the P(AN-VAc)/PE membrane and its GPE based on 1 M $LiPF_6$ in dimethyl carbonate/diethylene carbonate/ethylene carbonate (1:1:1 in volume) were investigated with a comparison of the unsupported P(AN-VAc) membrane. It is found that the P(AN-VAc)/PE membrane shows better mechanical strength and pore structure for electrolyte uptake than the P(AN-VAc) membrane, and subsequently the GPE based on P(AN-VAc)/PE exhibits higher ionic conductivity and electrochemical stability on cathode than the GPE based on P(AN-VAc). With the support of the non-woven fabric, the ionic conductivity of the GPE at room temperature increases from 1.4 to 3.8 mS cm^{-1}, the oxidation decomposition potential of the GPE on a stainless steel is improved from 5.0 to 5.6 V (vs. Li/Li^{+}). The mesocarbon microbeads (MCMB)/$LiMn_2O_4$ battery using P(AN-VAc)/PE as separator retains 94% of its initial discharge capacity after 100 cycles at *C*/2 rate, showing that the P(AN-VAc)/PE membrane is a possible alternative to the expensive separator for current liquid lithium ion battery.

Keywords Poly(acrylonitrile-vinyl acetate) · Support · Non-woven fabric · Gel polymer electrolyte · Lithium ion battery

1 Introduction

Lithium ion battery has been widely used in portable electronic devices, but its safety needs to be improved, especially for use in electric vehicles. The safety problem results mainly from the use of flammable liquid organic electrolyte and can be solved by substituting solid polymer electrolyte for liquid electrolyte. However, the low ionic conductivity of the solid polymer electrolyte cannot meet the requirement of rate charge/discharge performance of lithium ion battery. Gel polymer electrolyte (GPE) combines the advantages of liquid electrolyte and solid electrolyte, showing an ionic conductivity of 10^{-3} S cm^{-1} at room temperature, and therefore is believed to be an ideal solution to the safety problem of lithium ion battery [1–5].

Even though various GPEs plasticized by liquid organic solvents eliminate the room-temperature conductivity limit of solid polymer, their mechanical strength is still not sufficient to allow high-speed battery manufacturing that would involve the lamination and packing processes. Therefore, a mechanical support is needed for GPEs. In the supported GPE, the support contributes its mechanical strength to the GPE and the polymer in GPE contributes its chemical stability and high affinity with polar solvents.

There have been several reports on the application of supported GPEs in lithium ion battery [6–11]. Among the supports that have been used, polyethylene (PE) non-woven fabrics are attractive because of their low-cost and good compatibility with GPE. Lee et al. [6] made a novel porous separator based on poly(vinylidene fluoride) (PVdF) and PE non-woven matrix for rechargeable lithium batteries, showing that PE non-woven matrix provided the separator with good mechanical strength and a thermal shut-down property. Song et al. [7] prepared a composite electrolyte composed of a blend of polyethylene glycol

---

X. Li · M. Rao · Y. Liao · W. Li (✉) · M. Xu
School of Chemistry and Environment and Key Laboratory
of Electrochemical Technology on Energy Storage and Power
Generation of Guangdong Higher Education Institutes,
South China Normal University, Guangzhou 510006, China
e-mail: liwsh@scnu.edu.cn

diacrylate (PEGDA) and poly(methyl methacrylate) (PMMA) with a non-woven fabric as support, showing that the support provided the GPE with not only a better mechanical strength but also better electrochemical performances.

In our previous report [1], it was found that that poly(acrylonitrile-vinyl acetate) (P(AN-VAc)) based GPE had appropriate ionic conductivity and good electrochemical stability. However, its mechanical strength needs to be improved for its application in lithium ion batteries. In this paper, we developed a new GPE based on P(AN-VAc) using PE non-woven fabric as support and demonstrated its performance for lithium ion battery use. As a cheap support is combined with P(AN-VAc) that has high affinity with liquid electrolytes, the battery performances are expected to be improved with cheap battery manufacturing.

2 Experimental

2.1 Preparation

The copolymer, P(AN-VAc), in which the mole ratio of AN (Sinopharm Chemical Reagent Co., Ltd, China) to VAc (Sinopharm Chemical Reagent Co., Ltd, China) is 7:3, was prepared by solution polymerization as previous report [1]. The prepared P(AN-VAc) copolymer was dissolved in anhydrous *N*,*N*-dimethylformamide (DMF, Sinopharm Chemical Reagent Co., Ltd, China) and coated on PE non-woven fabric (Germany, 36 μm thick) to prepare a P(AN-VAc)/PE membrane. As shown in Fig. 1, PE non-woven fabric was immersed in the P(AN-VAc) solution, then the coated PE non-woven fabric was passed through a bath that was filled with distilled water to induce phase inversion, and dried at 100 °C to remove the residual solvent. To prepare the GPE, the P(AN-VAc)/PE membrane was transferred into a glove box (Supper1220/750, Belgium) and soaked with 1 M $LiPF_6$ in dimethyl carbonate (DMC)/diethylene carbonate (DEC)/ethylene carbonate (EC) (1:1:1 in volume, Guangzhou Tinci High-Tech Materials Co., Ltd., battery grade) for 1 h. For a comparison, the unsupported GPE was prepared by phase inversion as previous report [1].

2.2 Characterization

The thermal stability of the copolymer was analyzed with thermogravimetric analyzer (NETZSCH STA 409 PC/PG). The morphology of the P(AN-VAc)/PE and P(AN-VAc) membranes was examined with scanning electron microscope (JEOL, JSM-6380LV, Japan). The Brunauer–Emmett–Teller (BET) gas adsorption analyses were carried out by nitrogen adsorption–desorption isotherms at 77 K using Micromeritics ASAP 2020 instrument. Samples were degassed at 50 °C in vacuum for 4 h before the measurement.

The electrolyte uptake and leakage of membranes were calculated according to:

$$\text{Uptake}\,(\%) = (W_2 - W_1)/W_1 \times 100\% \tag{1}$$

$$\text{Leakage}\,(\%) = (W_2 - W_0)/(W_2 - W_1) \times 100\% \tag{2}$$

where W_1 and W_2 are the mass of the dry and the wet membrane, respectively; W_0 is the equilibrium weight of the membrane after absorbing the liquid electrolyte by putting the polymer membrane between two pieces of filter paper with a weight of 100 g on the top of the upper filter paper [12].

In the determination of the ionic conductivity, the GPE was sandwiched between two parallel stainless steel (SS) discs (diameter $\Phi = 16$ mm). The ionic conductivity was calculated from the bulk electrolyte resistance (R) according to:

$$\sigma = l/RS \tag{3}$$

where l is the thickness of the GPE, and S is the contact area between GPE and SS disc.

The lithium ion transference numbers (t_+) of GPE were determined by the combination of chronoamperometry

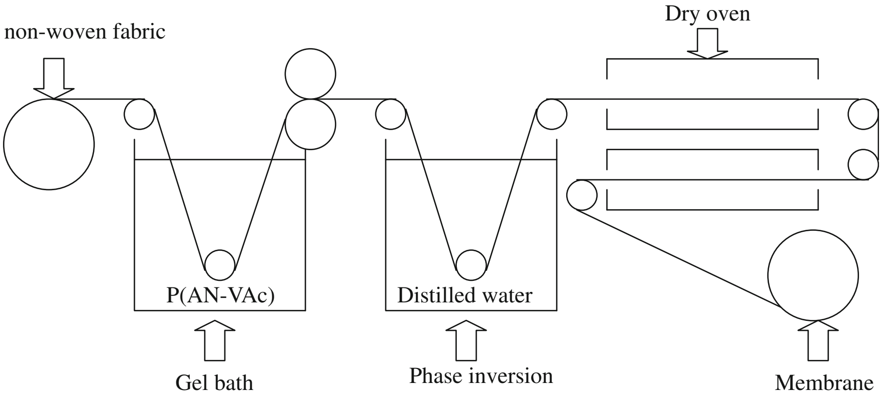

Fig. 1 Preparation schematic of PE non-woven fabric-supported P(AN-VAc) membrane

(CA) and electrochemical impedance spectroscopy (EIS) using the cell Li/GPE/Li. The t_+ was calculated based on [13, 14]:

$$t_+ = I_S(\Delta V - I_0R_0)/I_0(\Delta V - I_SR_S) \tag{4}$$

where I_0, I_S and ΔV are the initial current, the steady-state current and the potential applied to the cell in CA, respectively, and R_0 and R_S are the initial interfacial resistance and the steady-state interfacial resistance obtained by EIS, respectively. In this work, the used ΔV was 10 mV.

The electrochemical stability of the GPE was examined by linear sweep voltammetry on the cell Li/GPE/SS. Prismatic batteries were assembled for battery performance determination, with $LiMn_2O_4$ (Guangzhou Tinci High-Tech Materials Co., Ltd.) as cathode and mesocarbon microbeads (MCMB) (Guangzhou Tinci High-Tech Materials Co., Ltd.) as anode. The battery MCMB/P(AN-VAc)/PE/$LiMn_2O_4$ was setup using P(AN-VAc)/PE membrane as the separator and then filled with liquid EC-based electrolyte as the manufacturing for conventional lithium ion battery. The galvanostatic charge/discharge performance was examined between 2.75 and 4.2 V with a charge/discharge instrument (PCBT-138-64D WUHAN LISUN).

Mechanical strength measurements were carried out with an instrument (Gotech GT-TS-2000), at a crosshead speed of 10 mm min^{-1}, using standard dumb bell type tensile bars as the testing samples. The tests were carried out at room temperature.

3 Results and discussion

3.1 Thermal stability

The thermal stability of the materials was analyzed by thermogravimetry under N_2 atmosphere from room temperature to 600 °C at a heating rate of 10 °C min^{-1}. Figure 2 presents the TGA curves of PE non-woven fabric, P(AN-VAc) and P(AN-VAc)/PE based GPE. It can be seen from Fig. 2a that PE non-woven fabric begins to decompose at about 400 °C and loses its weight completely at about 500 °C. This suggests that PE non-woven fabric is stable up to 400 °C and decomposes to carbon dioxide and water when the temperature is higher than 500 °C. Figure 2b shows that P(AN-VAc) begins to decompose at about 300 °C but retains about 50% of its primary weight at 500 °C, indicating that P(AN-VAc) is stable up to 300 °C and its decomposition involves only the breakdown of partial bonds in its molecule rather than the formation of carbon dioxide even if the temperature is higher than 500 °C. Comparing Fig. 2c with Fig. 2b, it can be found that there is a weight loss of about 5% from 100 from 300 °C for the solvent evaporation and the decomposition temperature of P(AN-VAc)/PE is the same as that of P(AN-VAc). Therefore, the GPE based on PE non-woven fabric supported P(AN-VAc) can be used in lithium ion battery with its good thermal stability.

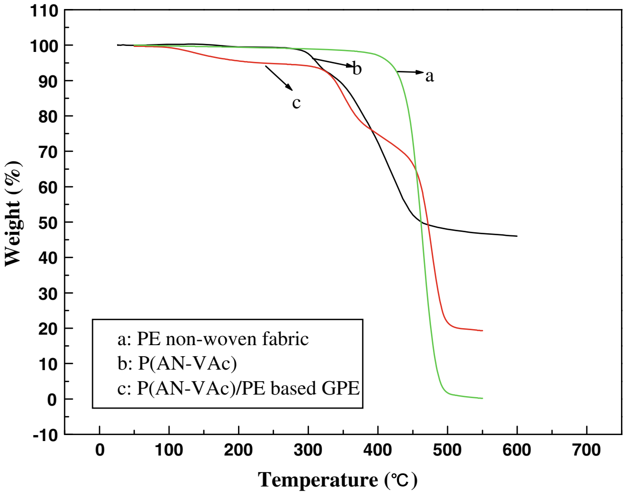

Fig. 2 TGA curves of PE non-woven fabric (*a*), P(AN-VAc) (*b*), and P(AN-VAc)/PE based GPE (soaked with 1 M $LiPF_6$ in DMC/DEC/EC (1:1:1 in volume)) (*c*) from room temperature to 600 °C at a heating rate of 10 °C min^{-1}

3.2 SEM images of support and membranes

Figure 3 presents the SEM images of the PE non-woven fabric, P(AN-VAc) and P(AN-VAc)/PE membranes. It can be seen from Fig. 3a that PE non-woven fabric is composed of different sizes of fibers which forms a non-uniform pore structure. The P(AN-VAc) membrane prepared by phase inversion exhibits a sparse pore structure, as shown in Fig. 3b. Differently, the P(AN-VAc)/PE membrane exhibits a dense pore structure with the pores cross-linked each others, indicating that the preparation method proposed in this paper (Fig. 1) can provide the membrane with good pore structure for the absorption of electrolyte.

Table 1 presents the pore parameters of the PE non-woven fabric, P(AN-VAc) and P(AN-VAc)/PE membranes obtained with BET analyses. It can been seen from Table 1 that the PE non-woven fabric membrane has a large average pore diameter but a small BET surface area and a small pore volume density. This pore structure of the PE non-woven fabric membrane is not suitable for lithium ion battery use because the large pores leads easily to the short circuit of the battery and the small pore volume density allows the low electrolyte absorptivity of the membrane that limits the rate performance of the battery. Similar to the observation by SEM, it can be known from Table 1 that P(AN-VAc)/PE membrane has better pore structure than the P(AN-VAc) membrane: the average pore diameter is smaller but the pore volume density is larger.

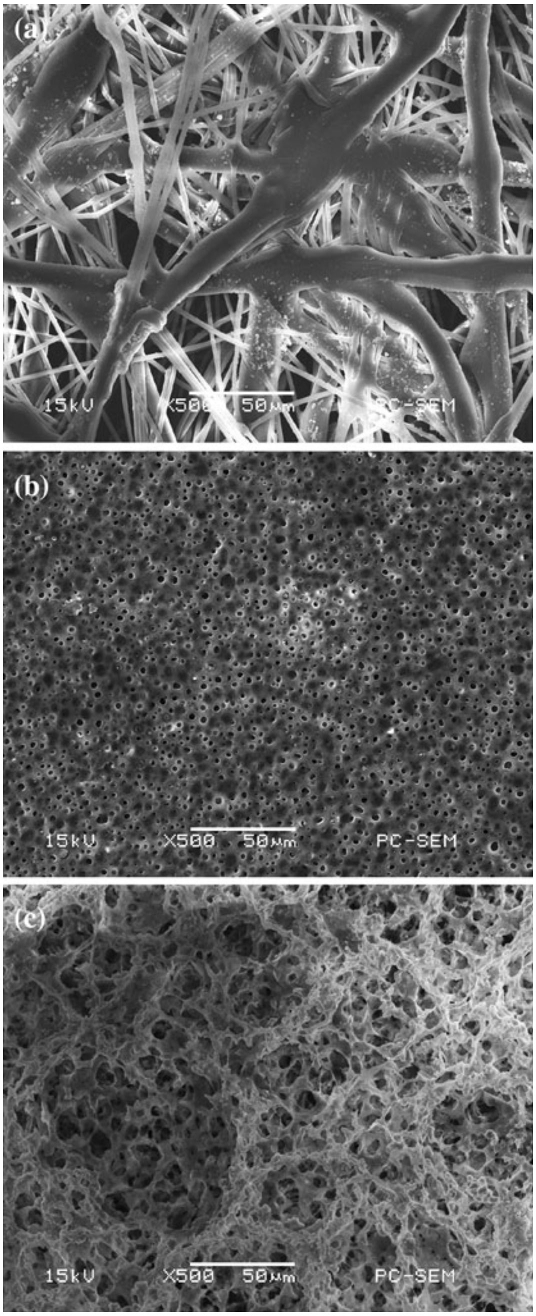

Fig. 3 SEM images of PE non-woven fabric [×500] (**a**), P(AN-VAc) membrane [×500] (**b**) and P(AN-VAc)/PE membrane [×500] (**c**)

Table 1 Pore parameters of P(AN-VAc)/PE, PE non-woven fabric and P(AN-VAc) membranes

Membrane	BET surface area ($m^2\ g^{-1}$)	Pore volume density ($mL\ g^{-1}$)	Average pore diameter (nm)
PE non-woven fabric	0.07	0.002	101
P(AN-VAc)	3.6	0.013	14
P(AN-VAc)/PE	20.6	0.048	10

It has been known that the presence of polar functional groups in P(AN-VAc) can provide the GPE with high ionic conductivity [15–17]. Moreover, the improved pore structure of the P(AN-VAc)/PE membrane must contributes to the ionic conductivity further, because the larger pore volume density can enlarge the contact areas between the polymer and electrolyte and retain much more electrolyte. Compared with the P(AN-VAc) based GPE, the P(AN-VAc)/PE based GPE is expected to provide lithium ion battery with better performances.

3.3 Ionic conductivity

Table 2 presents the electrolyte uptake of PE non-woven fabric and P(AN-VAc)/PE membranes and the ionic conductivity of the corresponding GPEs. It can be seen from Table 2 that the poor pore structure of the PE non-woven fabric membrane results in its lower electrolyte uptake and therefore the lower ionic conductivity of the corresponding GPE. Oppositely, the good pore structure of the P(AN-VAc)/PE membrane results in its high electrolyte uptake, leading to the high ionic conductivity of the P(AN-Vic)/PE based GPE, 3.8, compared to the 1.4 mS cm^{-1} of the P(AN-VAc) based GPE at room temperature.

The dependence of ionic conductivity (σ) for P(AN-VAc)/PE and P(AN-VAc) based GPEs on temperature from 25 to 75 °C is shown in Fig. 4. It can be seen from Fig. 4 that the $\log\sigma \sim 1/T$ curves for both GPEs exhibits a linear relationship, suggesting that conductive behavior of two GPEs obeys Arrhenius equation:

$$\sigma = \sigma_0 \exp(-E_a/RT) \tag{5}$$

where R is the gas constant, σ_0 the pre-exponential index and T the testing absolute temperature [12, 18–20]. Therefore, the activation energy for ion transportation can be calculated from the slope of the straight line according to Eq. 5. It is 12.9 kJ mol^{-1} for P(AN-VAc)/PE based GPE and 24.6 kJ mol^{-1} for P(AN-VAc) based GPE. This

Table 2 Properties of P(AN-VAc)/PE, PE non-woven fabric and P(AN-VAc) membranes and their GPEs

Membrane/GPE	Electrolyte uptake (wt%)	Ion conductivity (mS cm^{-1})	Transference number (t_+)	Mechanical strength (MPa)
PE non-woven fabric	160	1.1		29
P(AN-VAc)	188	1.4	0.36	15
P(AN-VAc)/PE	380	3.8	0.52	32

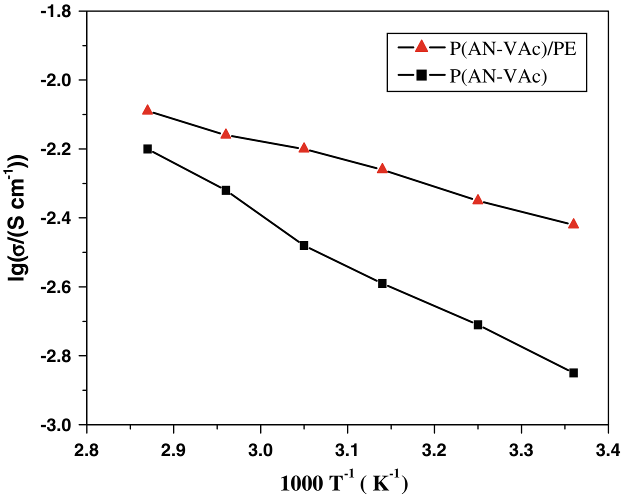

Fig. 4 Temperature dependence of ionic conductivity of P(AN-VAc) and P(AN-VAc)/PE based GPEs (soaked with 1 M $LiPF_6$ in DMC/DEC/EC (1:1:1 in volume))

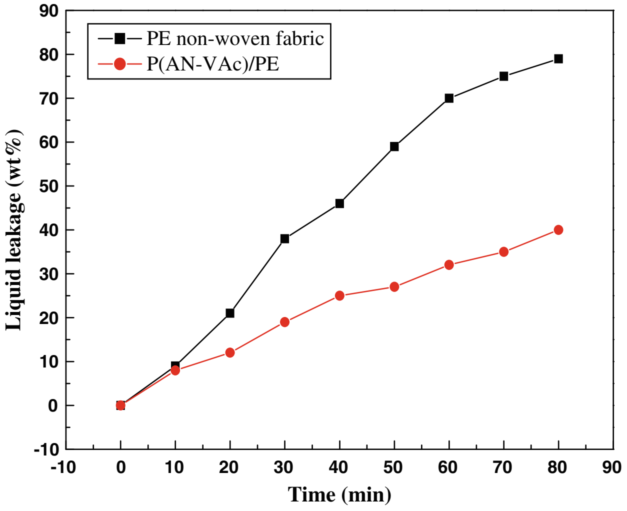

Fig. 5 Variation of electrolyte leakage of PE non-woven fabric and P(AN-VAc)/PE membranes (soaked with 1 M $LiPF_6$ in DMC/DEC/EC (1:1:1 in volume)) with time

suggests that there is a faster ion transportation in P(AN-VAc)/PE based GPE than in P(AN-VAc) based GPE.

The lower activation energy for ion transport in P(AN-VAc)/PE based GPE should be related to the improved pore structure of the P(AN-VAc)/PE membrane. The larger pore volume density of the membrane favors the ion transportation in the GPE. On the other hand, the larger BET surface area favors the segmental motion in the polymer, which results in an increase in the free volume of the system and contributes to the faster ion transportation [21, 22].

The affinity between membrane and electrolyte in a GPE can be illustrated based on the measurement of the electrolyte leakage of the membrane [23]. Figure 5 presents the variation of the electrolyte leakage of PE non-woven fabric and P(AN-VAc)/PE membranes with time. It can be seen from Fig. 5 that there is slower electrolyte leakage for the P(AN-VAc)/PE membrane than the PE non-woven fabric membrane. This indicates that the P(AN-VAc)/PE membrane has better affinity with the electrolyte than the PE non-woven fabric membrane. The better affinity between P(AN-VAc)/PE membrane and electrolyte should be ascribed to the good interaction between P(AN-VAc) and electrolyte.

3.4 Transference number

The ideal value of transference number (t_+) is one, since the t_+ lower than one would tend to develop concentration gradients near electrode surfaces [24]. However, due to the interaction between solvent molecules and lithium ions in electrolyte, the t_+ in electrolyte is always lower than one. It can be seen from Table 2 that the transference number in the P(AN-VAc)/PE based GPE is 0.52, higher than that of the P(AN-VAc) based GPE, which is only 0.36. This suggests that the lithium ion transference number of P(AN-VAc) based GPE can be improved by the support of non-woven fabric. The cross-linked pores in P(AN-VAc)/PE GPE acts as bridges, as shown in Fig. 3, which facilitates the transference of lithium ions in electrolyte.

3.5 Electrochemical stability

The electrochemical stability of electrolyte in a battery is its electrochemical widow which is reflected by the reduction and oxidation decomposition potentials on anode and cathode, respectively. In lithium ion battery, the reduction decomposition of electrolyte can be negligible because a stable solid state interface film is formed on anode. On the other hand, the oxidation decomposition of electrolyte on cathode when charging the battery is the main cause for safety problem of the battery. The electrochemical stability of electrolyte on the cathode of lithium ion battery can be understood by its oxidation behavior on an SS electrode [10, 11].

Figure 6 presents the linear voltammograms obtained from the cell Li/SS. It can be seen from the curves (a) of Fig. 6 that PE non-woven fabric based electrolyte begins to decompose at about 4.5 V (vs. Li/Li^+). Compared with PE non-woven fabric based electrolyte, P(AN-VAc) based GPE shows its better stability, as shown from the curve (b) of Fig. 6. The better stability of the P(AN-VAc) based GPE results from the interaction between the solvent molecules and the P(AN-VAc) polymer, while the solvent molecules in PE non-woven fabric based electrolyte are free and more easy to be oxidized.

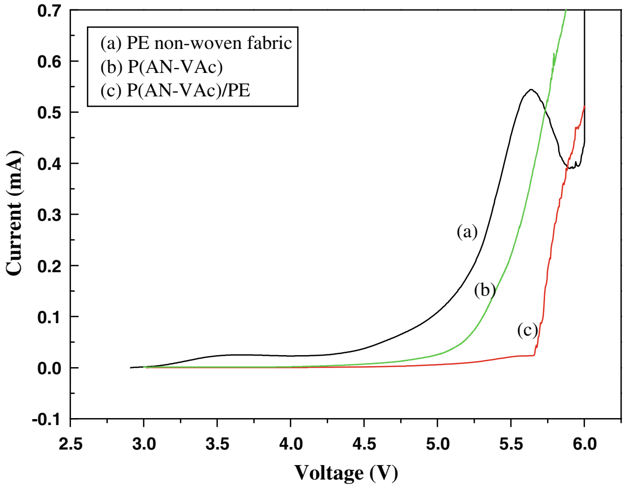

Fig. 6 Linear voltammograms on stainless steel for GPEs based on PE non-woven fabric (*a*), P(AN-VAc) (*b*) and P(AN-VAc)/PE (*c*), soaked with 1 M $LiPF_6$ in DMC/DEC/EC (1:1:1 in volume). Scan rate: 1 mV s^{-1}

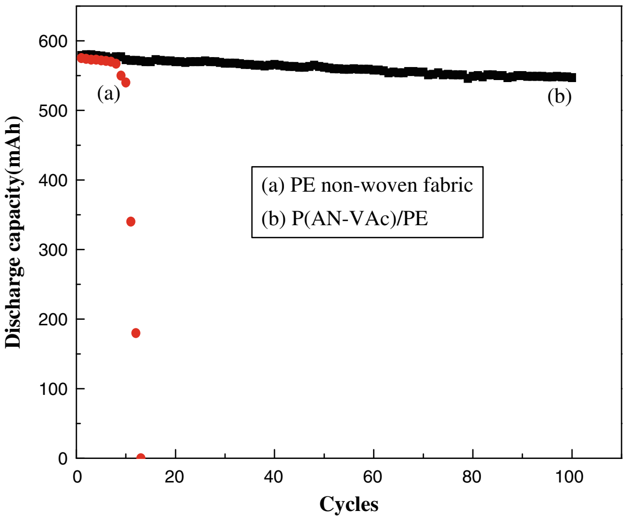

Fig. 7 Cycling performances of MCMB/$LiMn_2O_4$ batteries using P(AN-VAc)/PE (*a*) and PE non-woven fabric (*b*) as separators, discharged at C/2 under room temperature

The decomposition potential of P(AN-VAc)/PE based GPE is 5.6 V (vs. Li/Li^+), as shown by the curve (c) of Fig. 6, compared to the 5.0 V of P(AN-VAc) based GPE, showing that the former has better electrochemical stability than the latter. The better stability of the P(AN-VAc)/PE based GPE can be ascribed to the better pore structure of the P(AN-VAc)/PE membrane which resulting in stronger combination between the solvent molecules and P(AN-VAc) polymer.

3.6 Battery performance

To determine the performance of P(AN-VAc)/PE based GPE in lithium ion battery, prismatic battery were assembled using $LiMn_2O_4$ as cathode and MCMB as anode. Figure 7 presents the cyclic stability of MCMB/$LiMn_2O_4$ batteries using P(AN-VAc)/PE membrane and PE non-woven as separators. The batteries were subjected to a preconditioning cycle, with a cut-off voltage of 4.2 V for the upper limit and 2.75 V for the lower limit, at a constant current *C*/10. It can be seen from Fig. 7 that MCMB/P(AN-VAc)/PE/$LiMn_2O_4$ exhibits a good cyclic stability, which has an initial capacity of 579 mAh and still has a capacity of 547 mAh after 100 cycles, keeping over 94% of its initial discharge capacity. On the other hand, the PE non-woven fabric cannot be used as the separator of lithium ion battery. The discharge capacity of MCMB/PE non-woven fabric/$LiMn_2O_4$ decreases abruptly after 10 cycles, as shown in Fig. 7. The abrupt capacity decay results from the internal short-circuit of the battery, which is caused by the large pores in PE non-woven fabric, as shown in Fig. 3a and Table 1. Apparently, the combination of P(AN-Vac) with PE non-woven fabric provides the membrane with an improved pore structure and thus improves the cyclic stability of the battery.

Figure 8 shows the discharge curves of MCMB/P(AN-VAc)/PE/$LiMn_2O_4$ at different current rates (0.5*C*, 1*C* and 3*C*). It can be seen from Fig. 8 that both the voltage and the capacity of the battery decrease gradually with increasing discharge rate but keep relatively high values. The battery keeps 95 and 82% of its 0.5*C* discharge capacity for the discharges at 1*C* and at 3*C*, respectively, showing that the P(AN-VAc)/PE membrane is suitable for lithium ion battery use. The cost for the battery manufacturing can be expected to be reduced if this P(AN-VAc)/PE is used as the separator for lithium ion battery, because the PE non-

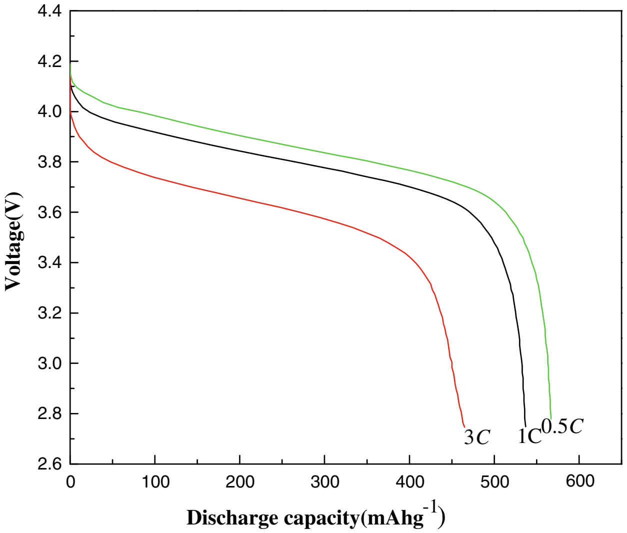

Fig. 8 Rate discharge performance of MCMB/P(AN-VAc)/PE/$LiMn_2O_4$ battery at room temperature

woven fabric is much cheaper than the commercial separators currently used in battery manufacturing.

3.7 Mechanical strength

The mechanical strength of the separator is important for battery performances, because weak separator is easy to degrade during battery manufacturing, resulting in the internal short-circuit of the battery. The fracture strength of PE non-woven fabric, P(AN-VAc) and P(AN-VAc)/PE membranes were measured and the results are shown in Table 2. It can be seen from Table 2 that the P(AN-VAc)/PE membrane has a fracture strength of 32 MPa at ambient temperature, higher than that of PE non-woven fabric membrane (29 MPa) and that of P(AN-VAc) membrane (15 MPa). It is obvious that the combination of P(AN-VAc) and PE non-woven fabric enforces each other. The enforced mechanical strength of the P(AN-VAc) is good for the manufacturing of lithium ion batteries. The fracture strength of the P(AN-VAc)/PE based GPE, with the P(AN-VAc)/PE membrane soaked in 1 M $LiPF_6$ in DMC/DEC/EC (1:1:1 in volume), was also measured. It is 27 MPa, a litter lower than the corresponding membrane, which can be ascribed to the weakened polymers (PE non-woven fabric as well as P(AN-VAc)) when they are soaked with solvents.

4 Conclusions

A cheap mechanical support, PE non-woven fabric, is simply impregnated with P(AN-VAc) copolymer and plasticized by liquid electrolytes, forming a good gel polymer electrolyte, P(AN-VAc)/PE based GPE. This GPE is mechanically and electrochemically stable and has an ionic conductivity of 3.8 mS cm^{-1} at room temperature. With the application of this GPE in lithium ion battery, the battery shows its good initial discharge capacity as well as its excellent cyclic stability. The synergistic results of the support PE non-woven fabric and the polymer P(AN-VAc) provides a cheap method for the manufacturing of lithium ion battery.

Acknowledgments This work was financially supported from National Natural Science Foundation of China (NNSFC, no. 20873046) and Specialized Research Fund for the Doctoral Program of Higher Education (Grant no. 200805740004).

References

1. Rao MM, Liu JS, Li WS, Liang Y, Liao YH (2009) J Power Sour 189:711
2. Zhang SS, Ervin MH, Xu K, Jow TR (2004) Electrochim Acta 49:3339
3. Liao YH, Zhou DY, Rao MM, Li WS, Cai ZP, Liang Y, Tan CL (2009) J Power Sour 189:139
4. Li ZH, Zhang P, Zhang HP, Wu YP, Zhou XD (2008) Electrochem Commun 10:791
5. Stolarska M, Niedzicki L, Borkowska R, Zalewska A, Wieczorek W (2007) Electrochim Acta 53:1512
6. Lee YM, Kim JW, Choi NS, Lee JA, Seol WH, Park JK (2005) J Power Sour 139:235
7. Song MK, Kim YT, Cho JY, Cho BW, Popov BN, Rhee HW (2004) J Power Sour 125:10
8. Kim DW, Oh B, Park JH, Sun YK (2000) Solid State Ion 138:41
9. Kritzer P (2006) J Power Sour 161:1335
10. Rao MM, Liu JS, Li WS, Liang Y, Zhou DY (2008) J Membr Sci 322:314
11. Rao MM, Liu JS, Li WS, Liao YH, Liang Y, Zhao LZ (2010) J Solid State Electrochem 14:255
12. Xiao Q, Wang X, Li W, Li Z, Zhang T, Zhang H (2009) J Membr Sci 334:117
13. Bruce PG, Vincent CA (1987) J Electroanal Chem 225:1
14. Evans J, Vincent CA, Bruce PG (1987) Polymer 28:2324
15. Kim JY, Lee Y, Lim DY (2009) Electrochim Acta 54:3714
16. Choe HS, Carroll BG, Pasquariello DM, Abraham KM (1997) Chem Mater 9:369
17. Akashi H, Tanaka K, Sekai K (1998) J Electrochem Soc 145:881
18. Xiao Q, Li Z, Gao D, Zhang H (2009) J Membr Sci 326:260
19. Gopalan AI, Santhosh P, Manesh KM, Nho JH, Kim SH, Hwang CG, Lee KP (2008) J Membr Sci 325:683
20. Wu F, Feng T, Bai Y, Wu C, Ye L, Feng Z (2009) Solid State Ion 180:677
21. Druger SD, Nitzam A, Ratner MA (1983) J Chem Phys 79:3133
22. Druger SD, Ratner MA, Nitzam A (1985) Phys Rev B 31:3939
23. Shi Q, Yu MX, Zhou X, Yan YS, Wan CR (2002) J Power Sour 103:286
24. Dias FB, Plomp L, Veldhuis JBJ (2000) J Power Sour 88:169